Inorganic Chemistry
Article

Inorg. Chem. **2009**, *48*, 11655–11659 **11655**
DOI: 10.1021/ic901760j

Formation of Hydrides in $(Ti_{1-x}Zr_x)Co_{2.00}$ $(0 < x < 1)$ Pseudobinary Alloys

H. T. Kuo,[†] R. S. Liu,*[,†] S. M. Filipek,*[,‡] R. Wierzbicki,[‡] R. Sato,[‡] C. L. Chan,[§] H. D. Yang,[§] and J.-F. Lee[∥]

[†]*Department of Chemistry, National Taiwan University, No. 1, Sec. 4, Roosevelt Road, Taipei 106, Taiwan,* [‡]*Institute of Physical Chemistry, Polish Academy of Sciences, 44/52 Kasprzaka, 01-224 Warsaw, Poland,* [§]*Department of Physics, National Sun Yat-Shen University, Kaoshiung 804, Taiwan, and* [∥]*National Synchrotron Radiation Research Center, Hsinchu 300, Taiwan*

Received September 4, 2009

The exposure of $(Ti_{1-x}Zr_x)Co_{2.00}$ intermetallic alloys to hydrogen at high pressure caused $(Ti_{1-x}Zr_x)Co_{2.00}$ (x = 0.50−0.90) hydrides in the alloy. The crystalline structural, electronic, and magnetic properties of parent alloys and of their hydrides were determined by using XRD (X-ray powder diffraction) and XAS (X-ray absorption spectrometry) and by the use of SQUID (a superconducting quantum interference device). Hydrogenation did not alter the crystal structure of the parent alloy, but it did increase the volume of the unit cell. An in situ Co *K*-edge XAS study of the hydride revealed that the valence state of Co increased during discharge (which is the release of hydrogen from the hydride). Hydrogenation of the parent alloy also reduced the magnetic moment. A possible mechanism of discharge for the hydride is also proposed.

Introduction

The use of hydrogen as an energy source is receiving increasing attention globally as the demand for environmentally clean fuels increases. Hydrogen, in particular, is a promising clean energy carrier. The main limitation on its use is the need to store it in a safe and practical manner. Therefore, materials for storing hydrogen are essential to future clean energy systems. Hydrogen can be stored in numerous forms, using various methods.[1−6] It can be stored in hydrogen-absorbing alloys[7] as a chemical hydride compound, such as $NaBH_4$[8,9] or $NaAlH_4$,[10] or in organic hydrides, such as methylcyclohexane or decalin.[11] Several researchers have focused on the synthesis and characterization of alloys that can contain hydrogen under moderate or high pressures at their crystal interstitial sites. In particular, the RM_2 (where R refers to a rare earth metal and M to a transition metal) group of Laves compounds are of interest because of not only their high H absorption but also their effect of hydrogen on their properties, including a considerable volume expansion and a change in their structural and magnetic properties. The effect of hydrogen absorption on the thermodynamic, structural, and magnetic properties of RM_2 with Laves phase compounds has been extensively investigated.[12,13] Our previous works have demonstrated that the reaction of hydrogen with $ZrFe_2$ and $ZrCo_2$ alloys under high-pressure hydrogen conditions results in the synthesis of $ZrFe_2H_4$ and $ZrCo_2H_2$ hydrides.[14] The structural and magnetic properties of these hydrides and the corresponding deuterides were subsequently examined using XRD (X-ray powder diffraction), NPD (neutron powder diffraction) and the Möessbauer spectrum measurements.[15,16] Both hydrides

*Corresponding author. Tel: +886-2-33661169. Fax: +886-2-23693121. E-mail: rsliu@ntu.edu.tw (R.S.L.); smf@ichf.edu.pl (S.M.F.).

(1) Dillon, A. C.; Jones, K. M.; Bekkedahl, T. A.; Kiang, C. H.; Bethune, D. S.; Heben, M. J. *Nature* **1997**, *386*, 377–379.
(2) Chahine, R.; Bose, T. K. *Int. J. Hydrogen Energy* **1994**, *19*, 161–164.
(3) Kojima, Y.; Suzuki, N. *Appl. Phys. Lett.* **2004**, *84*, 4113–4115.
(4) Ye, Y.; Ahn, C. C.; Witham, C.; Fultz, B.; Liu, J.; Rinzler, A. G.; Colbert, D.; Smith, K. A.; Smalley, R. E. *Appl. Phys. Lett.* **1999**, *74*, 2307–2309.
(5) Chambers, A.; Park, C.; Baker, R. T. K.; Rodriguez, N. M. *J. Phys. Chem. B* **1998**, *102*, 4253–4256.
(6) Ahn, C. C.; Ye, Y.; Ratnakumar, B. V.; Witham, C.; Bowman, R. C.; Fultz, B. *Appl. Phys. Lett.* **1998**, *73*, 3378–3380.
(7) Tamura, T.; Tominaga, Y.; Matumoto, K.; Fuda, T.; Kuriiwa, T.; Kamegawa, A.; Takamura, H.; Okada, M. *J. Alloys Compd.* **2002**, *330−332*, 522–525.
(8) Amendola, S. C.; Sharp-Goldman, S. L.; Janjua, M. S.; Kelly, M. T.; Petillo, P. J.; Binder, M. *J. Power Sources* **2000**, *85*, 186–189.
(9) Kojima, Y.; Suzuki, K.; Fukumoto, K.; Sasaki, M.; Yamamoto, T.; Kawai, Y.; Hayashi, H. *Int. J. Hydrogen Energy* **2002**, *27*, 1029–1034.
(10) Bogdanović, B.; Schwickardi, M. *J. Alloys Compd.* **1997**, *253−254*, 1–9.
(11) Newson, E.; Haueter, Th.; Hottinger, P.; VonRoth, F.; Scherer, G. W. H.; Schucan, Th. H. *Int. J. Hydrogen Energy* **1998**, *23*, 905–909.
(12) Yvon, K.; Fischer, P. In *Hydrogen in Intermetallic Compounds I, Topics in Applied Physics*, Vol. *63*; Schlapbach, L. Ed.; Springer Verlag: Berlin, Germany, 1988; pp 139−217.
(13) Fukai, Y. *The Metal−Hydrogen System*, Springer Verlag, Berlin, Germany,1993.
(14) Filipek, S. M.; Jacob, I.; Paul-Boncour, V.; Percheron-Guegan, A.; Marchuk, I.; Mogilyan- ski, D.; Pielaszek, J. *Pol. J. Chem.* **2001**, *75*, 1921–1939.
(15) Filipek, S. M.; Paul-Boncour, V.; Percheron-Guegan, A.; Jacob, I.; Marchuk, I.; Dorogova, M.; Hirata, T.; Kaszkur, Z. *J. Phys.: Condens. Matter* **2002**, *14*, 11261–11264.
(16) Paul-Boncour, V.; Bouree-Vigneron, F.; Filipek, S. M.; Marchuk, I.; Jacob, I.; Percheron- Guegan, A. *J. Alloys Compd.* **2003**, *356−357*, 69–72.

Published on Web 11/17/2009

are of interest because of their potential application as hydrogen-storing materials. However, such titanium compounds as TiFe, TiCo, and TiNi, all with CsCl-type structures, are well-known to be good hydrogen absorbers,[17,18] whereas Ti-based alloys of $TiFe_2$ and $TiCo_2$ are supposed to be nonhydride forming.[19] To prove that whether $TiCo_2$ can also be transformed into hydride at a sufficiently high hydrogen pressure, a series of pseudobinary $(Ti_{1-x}Zr_x)Co_{2.00}$ ($0 < x < 1$) alloys were investigated. In this study, $(Ti_{1-x}Zr_x)Co_{2.00}$ ($0 < x < 1$)-based hydrides were synthesized and characterized by such in situ methods as X-ray diffraction (XRD) and X-ray absorption spectrum (XAS) and by a superconducting quantum interference device (SQUID).

Experimental Section

Preparation of $(Ti_{1-x}Zr_x)Co_{2.00}$ Alloy and Hydride. $(Ti_{1-x}Zr_x)Co_{2.00}$ alloys with $x = 0.10$, 0.50, 0.75, and 0.90 were prepared by an arc-melting method using a nonconsumable tungsten electrode and a water-cooled copper tray in an atmosphere of argon. Zirconium (with a purity of 99.95%), iron (with a purity of 99.95%) and cobalt (with a purity of 99.95%) were utilized as starting materials. The alloys were remelted three times to ensure their high homogeneity. Then the melted buttons were sealed in evacuated quartz tubes for further homogenization by annealing at 850 °C for seven days and were cooled down and crushed into small pieces. Treatment with hydrogen at higher pressure, 1.0 GPa H_2, was performed using a piston-cylinder apparatus, described elsewhere.[14] The temperature range was from 25 to 100 °C. Following the treatment with hydrogen, the high-pressure apparatus was cooled to −10 °C, and the samples were moved out and placed in liquid nitrogen to prevent the desorption of hydrogen.

Methods of Characterizing Samples. The phases of the prepared samples were identified by powder X-ray diffractometry (XRD) using a PANalytical X'Pert PRO diffractometer. The diffraction intensity of the parent alloy was measured from 20 to 80° in steps of 0.02° for 10 s per step. The hydride was measured from 41 to 45° in steps of 0.05° for 10 s per step. Rietveld refinement was conducted using the general structure analysis system (GSAS) program to yield the parameters of the crystalline structure.[20]

Co *K*-edge X-ray absorption experiments were performed at the BL17C Wiggler beamline of the National Synchrotron Radiation Research Center (NSRRC) in Hsin-Chu, Taiwan. The electron storage ring was operated at an energy of 1.5 GeV with a beam current of 300 mA. A Si(111) double-crystal monochrommator was utilized to select the energy with a resolution ($\Delta E/E$) of 2×10^{-4}. The data were recorded at room temperature in the transmission mode using gas-filled ionization chambers. The ion chambers that were adopted to measure the incident (I_0) and transmitted (I_t) beam intensities were filled with a mixture of N_2 and H_2 gases and a mixture of N_2 and Ar gases, respectively. Energy calibration was performed based on the first inflection point of the Co *K*-edge (7709.0 eV) absorption spectrum of the Co metal foil as a reference. Reference spectra were simultaneously obtained for every in situ spectrum using Co metal foils. After the background had been subtracted out, the X-ray absorption near edge structure (XANES) spectra were normalized with respect to the edge jump.

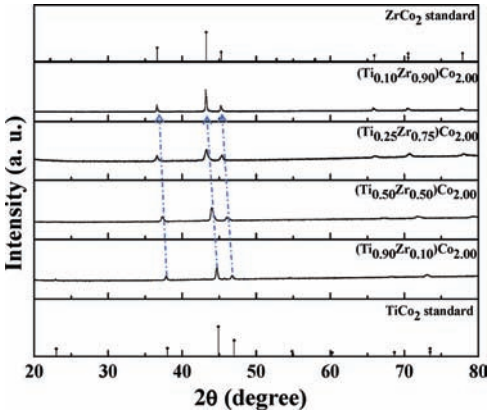

Figure 1. XRD patterns of $(Ti_{1-x}Zr_x)Co_{2.00}$ ($0 < x < 1$) alloys synthesized with various amounts of Zr dopant using an arc-melting method.

To determine hydrogen content in all hydrides, elemental CHN analysis was performed using the Haraeus CHN-O Rapid analyzer.

Magnetic hysteresis of $(Ti_{1-x}Zr_x)Co_{2.00}$ ($0 < x < 1$) alloys and hydride were measured using a SQUID magnetometer (Quantum Design, MPMS-XL7) in an applied magnetic field of 40 000 to −40 000 Oe at 300 K.

Results and Discussion

The substitution of Zr at the Ti sites did not change the structure of the alloys. The XRD profiles of the $(Ti_{1-x}Zr_x)Co_{2.00}$ ($0 < x < 1$) samples were obtained at room temperature and are presented in Figure 1. The fundamental reflections in the XRD patterns of $(Ti_{1-x}Zr_x)Co_{2.00}$ ($0 < x < 1$) correspond to those observed in the C15-type structure (space group, $Fd\bar{3}m$). Substitution of zirconium for titanium in the $(Ti_{1-x}Zr_x)Co_{2.00}$ solid solutions increases the lattice parameter. This behavior is similar to that of $(Ti_{1-x}Zr_x)Mn_2$ and $(Ti_{1-x}Zr_x)Fe_2$ systems,[21] whose lattice parameters increase with Zr content, causing the 2θ value of the XRD to shift downward, as indicated by the dashed arrow in the Figure 1.

Figure 2a displays the Rietveld refinement of $(Ti_{0.50}Zr_{0.50})Co_{2.00}$. All diffraction peaks were indexed to a cubic system with the space group $Fd\bar{3}m$. The structure of $(Ti_{0.50}Zr_{0.50})Co_{2.00}$ is calculated and presented in the inset in Figure 2a. Table 1 presents the lattice parameters obtained after refinement. The lattice parameters of $TiCo_2$, given by Wallbaum et al.,[22] were used as a reference. This finding is associated with the increase in the unit cell volume upon the substitution of Zr, which has a larger covalent radius, (1.45 Å) at the Ti (1.32 Å) sites, as presented in Figure 2b. The main effect is a smooth increase in the cell volume with x, which is accompanied by an expansion of the cubic lattice. The size of unit cell of $(Ti_xZr_{1-x})Co_{2.00}$ varies linearly with the composition, according to Vegard's law.

During the formation of hydrides, the lattice parameter of the parent alloy increases, shifting the XRD peaks to lower angles, as indicated by the arrow in Figure 3. At a hydrogen pressure of 1 GPa, the hydrides formed only in $(Ti_{0.10}Zr_{0.90})Co_{2.00}$, $(Ti_{0.25}Zr_{0.75})Co_{2.00}$, and $(Ti_{0.50}Zr_{0.50})Co_{2.00}$, according to XRD analysis. No hydride was stable, and all the hydrogen was released at 25 °C over several hours. The

(17) Yamanaka, K.; Saito, H.; Someno, M. *Nippon Kagaku Kaishi* **1975**, *8*, 1267–1269.
(18) Nambu, T.; Ezaki, H.; Yukawa, H. *J. Alloys Comp.* **1999**, *293*−*295*, 213–216.
(19) Zotov, T.; Movlaev, E.; Mitrokhin, S. *J. Alloys Comp.* **2008**, *459*, 220–224.
(20) Larson, A. C.; Von Dreele, R. B. *General Structure Analysis System (GSAS), Los Alamos National Laboratory Report*, Los Alamos National Laboratory: Los Alamos, NM, **2004**, 86−748.
(21) Bla Žina, Ž.; Trojko, R. *J. Less-Common Met.* **1987**, *133*, 277–286.
(22) Wallbaum, H. J.; Witte, H. *Z. Metallkd.* **1939**, *31*, 185–189.

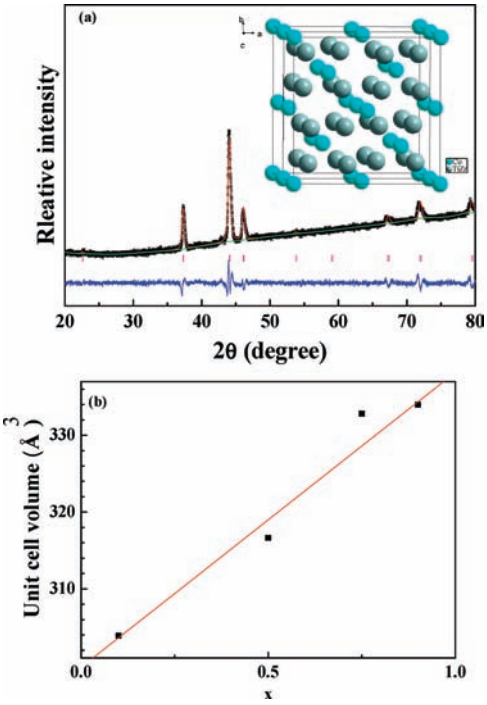

Figure 2. (a) Rietveld refinement of $(Ti_{0.50}Zr_{0.50})Co_{2.00}$. Observed (+) and calculated (red line) diffractogram for $Fd\bar{3}m$ model neglecting texture. Vertical pink tick marks indicate the peak positions of $(Ti_{0.50}Zr_{0.50})Co_{2.00}$. The bottom blue curve shows the difference between observed and calculated data on the scale of the diffractogram; (b) unit cell volume of C15 Laves phase in $(Ti_{1-x}Zr_x)Co_{2.00}$ $(0 < x < 1)$.

Table 1. Atomic Positions, Isotropic Thermal Factors, Occupancies, and Reliability Factors for Refinements of $(Ti_{0.50}Zr_{0.50})Co_{2.00}$ Phases in the Cubic $Fd\bar{3}m$ Space Group[a]

atoms	*x*	*y*	*z*	occupancy	Uiso (Å^2)
Co	0	0	0	16	0.025
Ti	5/8	5/8	5/8	8	0.025
Zr	5/8	5/8	5/8	8	0.025
space group: $Fd\bar{3}m$ (cubic)				reliability factors	
cell parameters:				R_p = 1.3%	
a = 6.8160 (2) Å				R_{wp} = 1.0%	
cell volume: 316.65 (2) Å^3				χ^2 = 1.04	

[a] From XRD data at 300 K.

hydrogen contents in all hydride samples were determined by CHN elementary analysis. The results in Table 2 reveal that the hydrogen content increased from 0.52 to 0.96 wt % as the Zr content increased. The formula of the hydride was also calculated. The hydrogen content in the hydride was consistent with an elementary analysis for increasing Zr content; the hydrogen value in the formula of related hydride increased from 0.88 to 1.97 as the Zr content increased from 0.25 to 0.90 in the formula of related parent alloys. This result is similar to those obtained by Zotov et al. for the $(Ti,Sc)Fe_2$ and $(Zr,Sc)Fe_2$ systems.[23] Based on this result, we believe that: (i) a pressure of 1 GPa was still too low to form the hydride in parent alloys with a high Ti concentration, or (ii) the hydride formed, but the discharge proceeded too rapidly and was hard to detect by XRD analysis.

The obtained maximum storage capacity of $(Ti_{0.10}Zr_{0.90})$-$Co_{2.00}$ is 0.96 wt % at 100 °C. To elucidate the effect of

(23) Zotov, T.; Movlaev, E.; Mitrokhin, S. *J. Alloys Comp.* **2008**, *459*, 220–224.

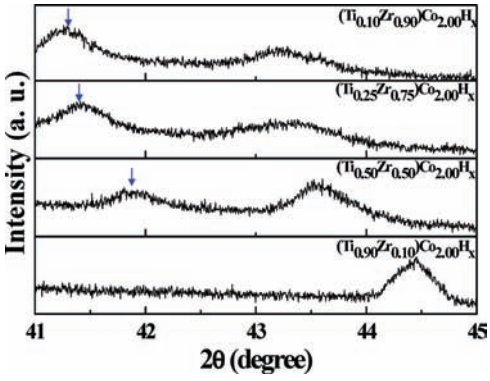

Figure 3. XRD patterns of $(Ti_{1-x}Zr_x)Co_{2.00}$ alloys following exposure to high hydrogen pressure of 1 GPa. XRD peaks of hydrides appear below 42 degrees, as indicated by an arrow, whereas peaks above 43 degrees are from the hydride or/and parent alloy.

Table 2. The Hydrogen Absorption Amounts of $(Ti_{1-x}Zr_x)Co_{2.00}$ Alloys

sample no.	elemental analysis of H wt %	calculated formula
x = 0.10	0.52	$(Ti_{0.90}Zr_{0.10})Co_{2.00}H_{0.88}$
x = 0.50	0.66	$(Ti_{0.50}Zr_{0.50})Co_{2.00}H_{1.23}$
x = 0.75	0.82	$(Ti_{0.25}Zr_{0.75})Co_{2.00}H_{1.63}$
x = 0.90	0.96	$(Ti_{0.10}Zr_{0.90})Co_{2.00}H_{1.97}$

zirconium doping on the discharge kinetics, the rates of discharge for the XRD peak ratios of hydride/parent alloy were measured, as displayed in Figure 4. Figure 4a presents the in situ XRD patterns of the discharging process of the $(Ti_{0.10}Zr_{0.90})Co_{2.00}$ hydride. The three sets of peak ratios of hydride/parent alloy peaks are designated I, II, and III. The positions of the XRD peak of the hydride are indicated by dotted lines; those of the parent alloy are indicated by dashed lines. The variation of peak position and of intensity for any hydride/parent alloy can be clearly identified. During the discharge process, the XRD signal of the hydride becomes less intense, while that of the parent alloy simultaneously increases. To determine the discharge kinetics of the hydride, Figure 4b plots the discharge curve (hydride/parent alloy ratio as a function of discharging time) calculated from set II of peak ratios of intensities in Figure 4a. Zirconium doping markedly promoted hydrogen absorption. The ratio of hydride/parent alloy in the original state for $Ti_{0.10}Zr_{0.90}Co_{2.00}$ is 1.16 and for $Ti_{0.10}Zr_{0.90}Co_{2.00}$ is 1.05. However, the discharge of the $(Ti_{1-x}Zr_x)Co_{2.00}$ $(0 < x < 1)$ system in the initial state became rapid as the amount of Zr dopant declined. Accordingly, only the samples with x = 0.75 and 0.90 are presented as examples. Figure 4b clearly indicates that doping significantly influences the kinetics of hydrogen release. The ratio of the hydride/parent alloy in the $(Ti_{0.10}Zr_{0.90})Co_{2.00}$ hydride is from 1.16 to 0.90 and the $(Ti_{0.25}Zr_{0.75})Co_{2.00}$ hydride is from 1.05 to 0.90 after 3.75 h of discharging. The discharging of $(Ti_{0.25}Zr_{0.75})Co_{2.00}$ hydride is faster, 96.3% (1.01/1.15), than that of $(Ti_{0.10}$-$Zr_{0.90})Co_{2.00}$ hydride, 92.1% (0.97/1.05). Zirconium doping greatly affects the absorption and release of hydrogen by $TiCo_2$. As the amount of Zr increases, discharging slows, suggesting that a longer time is required to overcome the deactivation energy, yielding a lower diffusion rate. Moreover, the escape velocity of hydrogen in the presence of more Zr in the $(Ti_{1-x}Zr_x)Co_{2.00}$ $(0 < x < 1)$ system may be lower, causing the discharging to take longer. This finding also

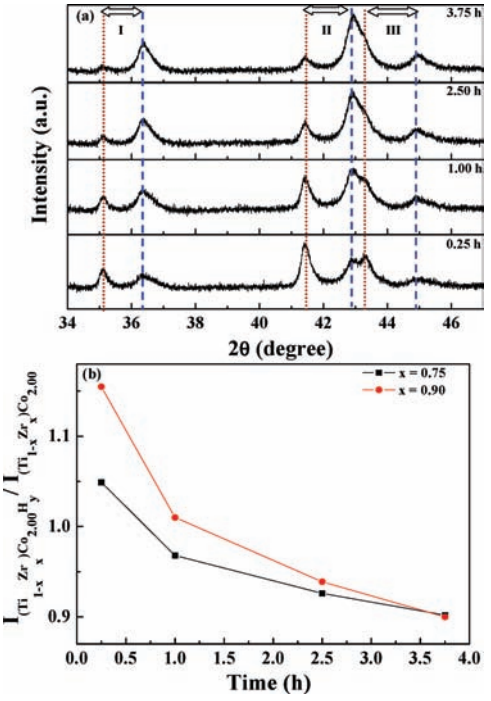

Figure 4. (a) In-situ XRD patterns of the discharge process of $(Ti_{0.10}Zr_{0.90})Co_{2.00}$ hydride upon exposure to ambient temperature at 25 °C. Three sets of hydride/parent alloys are denoted I, II, and III. Dotted line represents the signal from the hydride, and dashed line is from the parent alloy. (b) Intensity ratio, $I_{(Ti1\text{-}xZrx)Co2Hy}/I_{(Ti1\text{-}xZrx)Co2}$, between two peaks for set II plotted against discharge time.

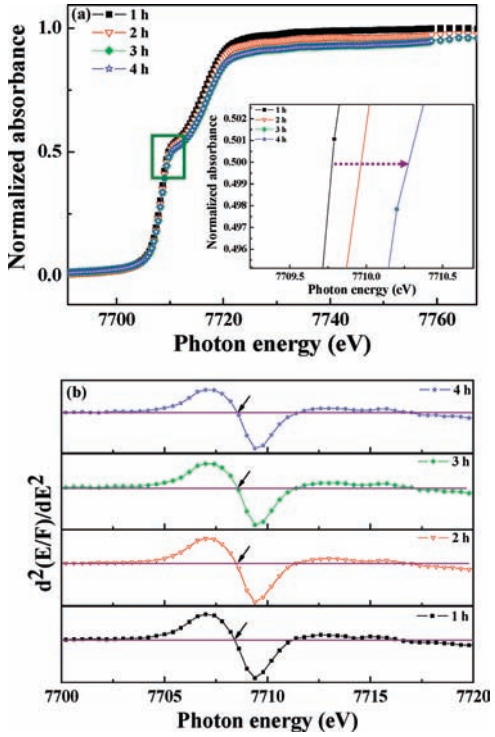

Figure 5. (a) In-situ XAS patterns at Co *K*-edge of the discharge process of $(Ti_{0.10}Zr_{0.90})Co_{2.00}$ hydride during exposure to ambient temperatures at 25 °C; the near-edge region is shown in the inset. (b) Second derivatives of normalized Co *K*-edge XAS spectra.

supports the result that $ZrCo_2$[14] forms a hydride more easily than does $TiCo_2$.[19]

Figure 5 displays in situ XAS spectra at the Co *K*-edge of $(Ti_{0.10}Zr_{0.90})Co_{2.00}$ hydride. To compare quantitatively the intensities of absorption features in various discharging states, the experimental Co *K*-edge spectra were normalized using the standard edge step normalization procedure. The background was subtracted from all XAS spectra, which were then normalized with respect to the edge jump. The absolute zero point of energy is taken with respect to the first point of inflection of the Co metal derivative spectrum (E_0), which corresponds to the excitation of an inner-shell electron to an empty state just above the Fermi edge of the Co metal. For each spectrum, Co foil was scanned to correct for the energy shift, such that energy-calibrated spectra were consistently obtained. In most related studies, the Co valence state is determined from the position of the absorption near edge (as displayed in the inset), which increases as the valence state increases. We suggest that as the $(Ti_{0.10}Zr_{0.90})Co_{2.00}$ hydride sample is discharged, the free electron is extracted from its electronic band, combined with H^+ to form hydrogen, and released from the surface of the hydride sample; the valence state of the cobalt metal is, thus, shifted from low to high energy. Figure 5a depicts the details. To clarify the edge features, only a small energy range of the XAS is presented. Figure 5b plots the second derivative function of the Co *K*-edge of the $(Ti_{0.10}Zr_{0.90})Co_{2.00}$ hydride sample for various discharging times. The zero crossing of the main absorption features, indicated by the arrow in Figure 5b, representing the inflection point energy was found to increase from 7708.4 to 7708.5 eV in 1−4 h. The curve of the second derivative of the Co *K*-edge at various discharging times has a similar shape. Figure 5b also presents the zero crossing of the main absorption features, which suggests that the local structure is mostly maintained during discharge.

Hydrogen atoms in the interstitial alloy increase the lattice parameters, significantly increasing the Co−Co distance, ultimately resulting in significant changes in the magnetic properties, which the Co−Co interatomic distance critically affect. In Figure 6a, the hydride of $(Ti_{0.10}Zr_{0.90})Co_{2.00}$ reduces magnetic susceptibility. Our earlier studies found a similar reduction in magnetic susceptibility in the YFe_2 hydride.[24] The volume effect is revealed by an increase in magnetization which is caused by increased localization of the 3d orbitals of Co. However, in hydrides, hydrogen dominates the volume expansion, reducing the magnetic moment. Figure 6b plots the results of using in situ SQUID to determine magnetic susceptibility during the discharge of $(Ti_{0.10}Zr_{0.90})Co_{2.00}$. Two distinct phases, hydride and solid solution in parent, are present during the discharge process; the hydrogen is released from the hydride, reducing the lattice parameter of the parent alloy. The magnetic susceptibility is increased and shifted back to that of the parent alloy, suggesting that the hydrogen can be reversibly stored in the proposed material.

The mechanism of charging/discharging follows the well-known process of metallic hydride formation, displayed in Figure 7. It comprises the following three equations:

$$H_{2(g)} \overset{\text{surface of host}}{\rightleftharpoons} H_{2(ad)} \quad (1)$$

(24) Paul-Boncour, V.; Matar, S. F. *Phys. Rev. B: Condens. Matter* **2004**, *70*, 184435-1−184435-8.

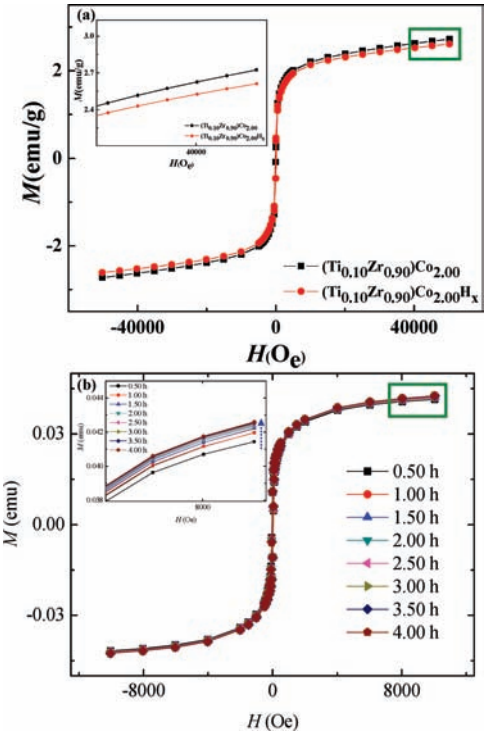

Figure 6. (a) Magnetization vs applied magnetic field curves of $(Ti_{0.10}Zr_{0.90})Co_{2.00}$ alloy and hydride samples at 5 K; (b) In situ magnetization vs applied magnetic field curve of $(Ti_{0.10}Zr_{0.90})Co_{2.00}$ hydride at 300 K.

$$H_{2(ad)} \rightleftharpoons 2H^{+}{}_{(ad)} + 2e^{-} \qquad (2)$$

$$2H^{+}{}_{(ad)} + 2e^{-} \underset{2e^{-}}{\overset{\text{Inner of host}}{\rightleftharpoons}} \text{2H-host} \qquad (3)$$

electron band of host

In hydrogenation (charging), the host is the pure metal or alloy, and the guest is the hydrogen. In eq 1, the hydrogen diffuses and adsorbs on the surface of the host. During heating to prepare the hydride, the hydrogen overcomes the surface potential of the host and breaks the H−H bond to form H^+ and e^-, as in eq 2. In eq 3, H^+ bonds to the host; e^- is injected into the electron band of the host and affects its electronic properties. The lattice parameter thus increases. The dehydrogenation (discharging) process is the opposite process in which hydrogenation (charging) is reversed.[25]

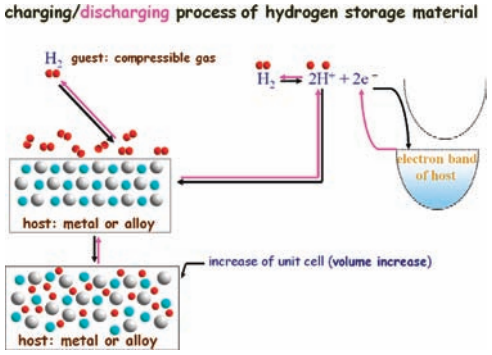

Figure 7. Proposed charging/discharging process.

Conclusions

$(Ti_{1-x}Zr_x)Co_{2.00}$ $(0 < x < 1)$ alloys and their hydrides were characterized by XRD, XAS, and SQUID. The XRD patterns reveal that both alloy and hydride, with a low diffraction angle, have a pure cubic phase. Rietveld refinement analysis demonstrates a remarkable increase in lattice parameter upon the doping of zirconium (1.45 Å) into the titanium (1.32 Å) sites of the crystal lattice. Despite a very high hydrogen pressure during the synthesis of the hydride, a fully charged $(Ti_{1-x}Zr_x)Co_{2.00}$ $(0 < x < 1)$ hydride was not obtained when x was lower than 0.50. The in situ XRD signal of the discharging of $(Ti_{0.10}Zr_{0.90})Co_{2.00}$ hydride declines, while that of the parent alloy increases. In situ cobalt *K*-edge XAS of the discharge process of $(Ti_{0.10}Zr_{0.90})Co_{2.00}$ hydride shows a shift in the absorption energy from low to high energy revealed by the valence state on cobalt metal atoms. The use of a SQUID to measure magnetization indicates that the magnetic moment decreases more after hydrogenation than that of the parent alloy. This fact follows from weakening of the Co−Co magnetic coupling and the filling up of the cobalt conduction band by electrons from hydrogen atoms. The in situ SQUID measurement of magnetization of $(Ti_{0.10}Zr_{0.90})Co_{2.00}$ hydride demonstrates that the magnetic change during the formation of hydrides is reversible.

Acknowledgment. The authors would like to thank the National Science Council of the Republic of China, Taiwan, for financially supporting this research under contract numbers NSC 97-2113-M-002-012-MY3 and 96-2113-M-002-014-MY2.

(25) Martin, M.; Gommel, C.; Borkhart, C.; Fromm, E. *J. Alloys Comp.* **1996**, *238*, 193–201.